Nonlinear Optical Susceptibility of a Model Guest-Host Polymeric System as Investigated by Electrooptics and Second-Harmonic Generation

T. Goodson III, S. S. Gong,† and C. H. Wang*

Department of Chemistry, University of Nebraska—Lincoln, Lincoln, Nebraska 68588-0304

Received December 7, 1993; Revised Manuscript Received April 7, 1994®

ABSTRACT: The magnitude and stability of the induced dipolar orientation of a nonlinear optical (NLO) chromophore doped in an amorphous polymeric matrix is investigated. The chromophores are aligned using electric field poling. The linear electrooptic (EO) Pockels effect and second-harmonic generation (SHG) techniques are used to probe the electric field-induced alignment. Both the Pockels coefficient and the second-order susceptibility show a nonlinear relationship with the NLO chromophore concentration. Using a relationship based on the two level model, the Pockels coefficient is compared with the second-order nonlinear susceptibility measured by SHG. The temperature dependence of the decay time constant of the SHG signal is found to follow an empirical relationship such as the Vogel-Tammen-Fulcher (VFT) equation. The decay time constant of the SHG signal is also found to be increasing with increasing chromophore concentration. This concentration dependence is interpreted as due to orientational pair correlation between chromophores and between chromophores and polymer chains.

I. Introduction

A primary impediment to the realization of the technological potential of poled polymers has been the lack of long-term temporal stability of the poled molecular order necessary for second-order NLO effects.[1,2] One method of improving thermal stability is to move away from guest-host polymer systems to polymers in which the nonlinear chromophore is covalently bound to the polymer either as a side chain or in the main chain.[3-5] Systems in which the oriented dye molecules are chemically incorporated into a highly cross-linked matrix while it is being electrically polarized have also been investigated.[6,7] Recently, striking stabilities of polar order at high temperatures have been demonstrated for high T_g polyimides simply doped with NLO chromophores.[8-10] Undoubtedly, guest-host systems hold an explicit advantage in synthetic directness, since they do not require chemical attachment. Investigation of a model guest-host system is thus of interest because it provides needed information regarding the orientational behavior of NLO chromophores in a polymer environment.

In this study both electrooptics (EO) and second-harmonic generation (SHG) are used to probe the orientational alignment of the NLO chromophores in a model guest-host system. In section II the experimental details are given. Section III shows the results of the Pockels effect and SHG study. In this section the conversion from the Pockels coefficient to the second-order susceptibility ($\chi^{(2)}$), measured at the second-harmonic optical frequency, is also considered. The temperature and concentration dependence of the relaxation of the SHG signal is considered, while also giving details of the effect of the electric field on the SHG intensity.

II. Experimental Section

Appropriate amounts of 4-(*N*,*N*-dimethylamino)-3-acetamidonitrobenzene (DAN) and poly(methyl methacrylate) (PMMA) were dissolved in chloroform to form solutions of different chromophore concentrations. The amount of chloroform in each solution was adjusted to give a desired viscosity suitable for spin coating. The solutions were filtered with 0.2-μm filters to remove undissolved particulates. Films were prepared by spin coating the polymer solution on soda lime glass slides, which were precoated with 300-Å SiO_2 and 250-Å ITO (indium tin oxide) films, using the sputtering technique. The NLO polymer/ITO sample assembly was placed in a vacuum oven at 40 °C for over 24 h to remove the solvent used in spin coating. The absence of solvent was checked with infrared spectroscopy after the baking process; no solvent IR absorption band could be detected. After certifying the chromophore concentration, another ITO glass slide was then placed on top of the polymer/ITO glass slide to form a sandwich configuration for electrode poling. The glass transition temperature (T_g) of the sample was determined by using DSC (differential scanning calorimeter, Perkin-Elmer Delta series). The glass transition temperature of the samples as a function of chromophore concentration is given in Table 1. The temperature rate was set at 10 °C per minute. The refractive index and thickness of the sample were determined by a prism coupler (Metricon) modified for the multiple wavelength operation. The prism coupler is operated in accordance with the optical waveguide principle where the polymer film serves as the propagation layer in the slab waveguide configuration. The refractive index dispersion for the film containing 5 wt % DAN dissolved in PMMA is shown in Figure 1. This dispersion can be fitted to the equation[11]

$$n(\lambda) = 1.47906 + (3102.6311)/(\lambda^2 - 2097.3845) \quad (1)$$

where λ is the wavelength in nanometers. Also included in Figure 1 is the refractive index concentration dependence for the DAN/PMMA system from 0 to 25 wt %, measured at the optical wavelength 632.8 nm.

The linear electrooptic measurements were made using a Mach-Zehnder interferometer apparatus constructed in our laboratory.[12] The incident light beam at 632.8 nm is polarized along the 1-axis (on the films surface) and propagates along the 3-axis normal to the film surface. The change in the refractive index due to applied electric fields is given by[13]

$$\Delta n = -n^3 r_{13} E_{ac}/2 \quad (2)$$

where E_{ac} is the applied ac electric field oscillating at frequency Ω. The ac field is along the 3-axis. The coefficient r_{13} is the linear electrooptic (or Pockels) coefficient, which is induced by the poling dc field, codirectional with the ac field. We have found that at elevated temperature r_{13} eventually decays to zero after the poling field is removed; but at ambient temperatures the magnitude of the coefficient remains comparably stable with

* Author to whom correspondence should be sent.
† Permanent address, Wuhan Institute of Physics, Chinese Academy of Science, Wuhan, China.
® Abstract published in *Advance ACS Abstracts*, June 1, 1994.

0024-9297/94/2227-4278$04.50/0

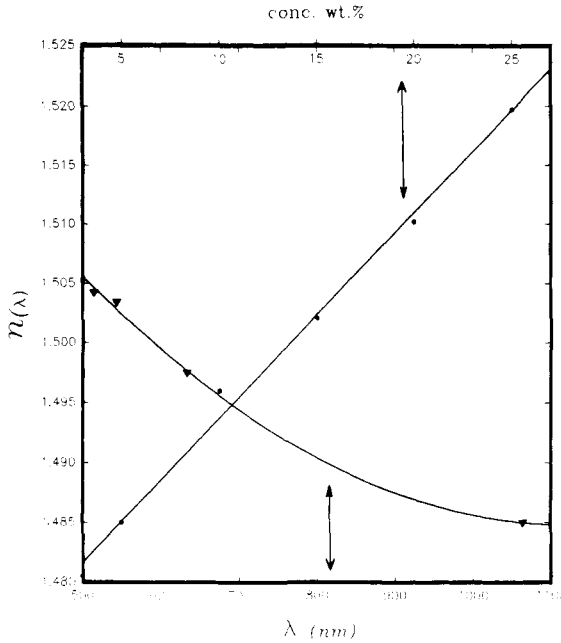

Figure 1. Concentration (●) and wavelength (▼) dependence of the refractive index of DAN dissolved in PMMA. The dispersion was measured with 5 wt % DAN.

Table 1. The Glass Transition Temperature (T_g), the Pockels Coefficient (r_{13}), and Second-Harmonic Coefficient (d_{13}) at Various Chromophore Concentrations

NLO conc (wt %)	EO: r_{13} (pm/V, ±0.03)	d_{13} (pm/V) SHG ±0.03	d_{13} (pm/V) calc	T_g (°C, ±)
3.3	0.07	0.11	0.105	94
4.9	0.11	0.26	0.24	87
10	0.18	0.55	0.41	79
14.8	0.38	1.11	1.01	71
21	0.53	1.31	1.24	59
24	0.61	1.45	1.43	52

only a minimal loss. To avoid any loss, the measurements reported here were carried out in the presence of the poling field. This result is similar to that found by Hirschmann[14] in the guest–host system.

The second-harmonic generation (SHG) was carried out using an apparatus similar to that reported by Guan and Wang.[15] It consists of an Nd:YAG laser (Spectra-Physics GCR-11, λ = 1.06 μm, Q-switched at 10 Hz), a computer-controlled goniometer stage, a series of short-pass and long-pass filters, a polarizer, a half-wave plate, a photomultiplier tube, and a boxcar integrator which was interfaced to a PC. The sample assembly mounted on the goniometer stage was placed in an oven which is temperature controlled to the accuracy of ±0.5 °C. The electric field poling was carried out inside the temperature-controlled oven. To obtain information of the time dependence of the signal decay, the electric field was switched off and the electrodes were shorted, after the sample signal had reached a stabilized steady state in a constant temperature environment.

The Maker fringe of a Y-cut single-crystal quartz plate (d_{11} = 0.5 pm/V) was used as a reference to determine the magnitude of the second-order susceptibility of the sample.

III. Results and Discussion

A. Linear Electrooptic Effect. The Pockels effect can be realized through the use of a Mach-Zehnder (MZ) interferometer.[12] A change in the refractive index results in the phase shift of the light beam traversing the material. The phase shift $\Delta\Phi(t)$ is modulated by the AC field at frequency Ω

$$\Delta\Phi(t) = A \cos \Omega t \tag{3}$$

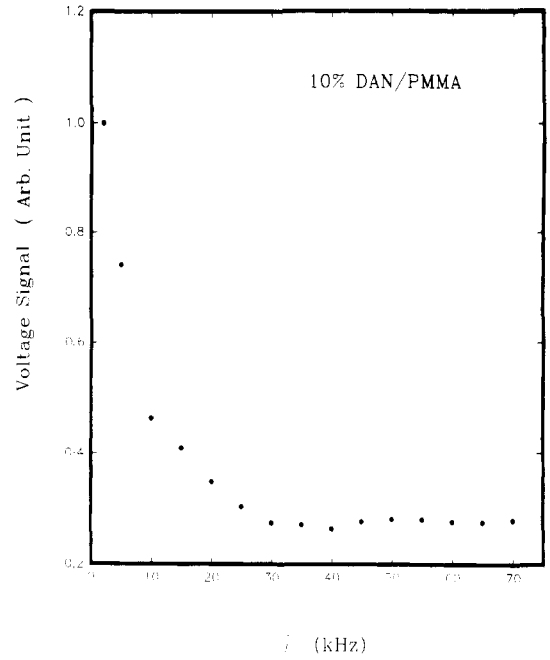

Figure 2. The electrooptical signal (●) from the Mach-Zehnder interferometer plotted as a function of the frequency of the applied AC field for 10 wt % DAN in PMMA. Note that the signal decreases rapidly with increasing frequency, and reaches a constant value after 30 kHz.

where A is the modulating amplitude given by

$$A = (\pi/\lambda)(n^3 r_{13} V_{ac}) \tag{4}$$

where the second identity is the result of eq 2. Thus the electrooptic coefficient can be calculated as long as the applied field, amplitude of the signal, and refractive index are all known.

It should be noted that the measurement of the EO coefficient is often complicated with unwanted artifacts, such as electrode attraction, mechanical resonance, and surface charge trappings.[16,17] In order to obtain a reliable r_{13} coefficient, these artifacts must be eliminated. To find the extent of these artifacts the response is measured at different frequencies of the AC field for a 10 wt % DAN/PMMA film; the result is shown in Figure 2. In this experiment the sample and the electrodes were set in a sandwich geometry. As it can be seen there is a relatively larger signal for frequencies less than 20 kHz. The response levels off at frequencies above 30 kHz. A similar result is seen when a gold film is evaporated onto the single polymer film, serving as another electrode. The large response below 20 kHz is due to electrode attraction and not the true electrooptical effect.

The linear EO effect was also measured as a function of concentration. The r_{13} values are given in Table 1 and also plotted in Figure 3 for six different NLO chromophore concentrations. The result shows that the EO coefficient increases with increasing chromophore concentration, but the increase is not linear with respect to the chromophore concentration.

Using the measured r_{13} values we have predicted the second-harmonic coefficient d_{13} using a two-level model relation given as[18,19]

$$\left|\frac{r_{13}}{d_{13}}\right| = \frac{4}{n^4(\omega)} \frac{\mathcal{F}^{\omega}\mathcal{F}^{\omega}\mathcal{F}^{0}}{\mathcal{F}^{2\omega'}\mathcal{F}^{\omega'}\mathcal{F}^{\omega'}} \frac{(3\omega_0^2 - \omega^2)(\omega_0^2 - \omega'^2)(\omega_0^2 - 4\omega'^2)}{3\omega_0^2(\omega_0^2 - \omega^2)^2} \tag{5}$$

where ω' is the frequency of the fundamental used in

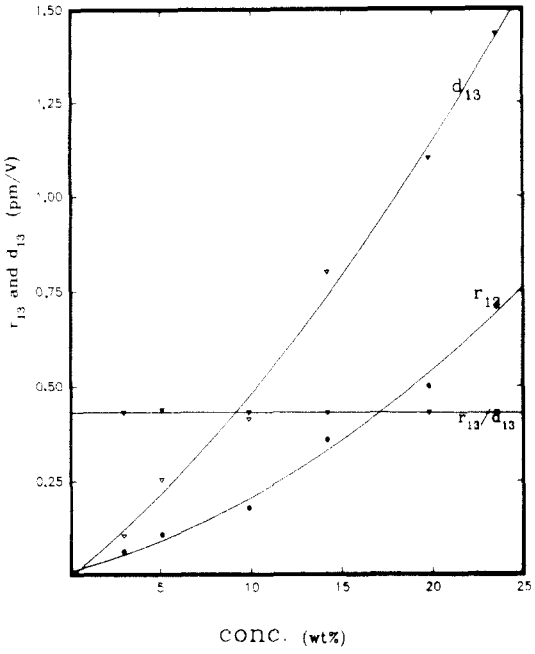

Figure 3. Measured Pockels coefficient r_{13} (●) and second-harmonic coefficient d_{13} (▼) plotted as a function of the DAN concentration in PMMA, the ratio of the coefficients (▼). The solid line going through the d_{13} data corresponds to calculated values using eq 5.

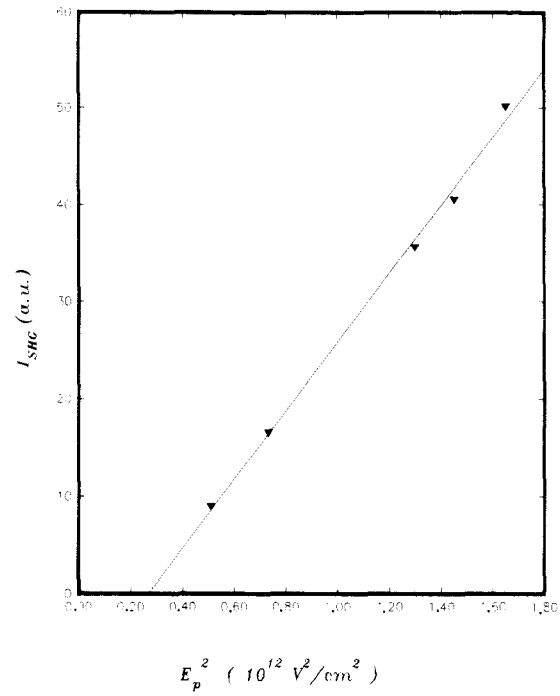

Figure 4. SHG signal (▼) plotted versus the square of the poling field strength E_p. The dotted line at low E_p shows that a threshold poling field is needed to induce a macroscopic polarization.

measuring d_{13} and the electrooptic coefficient is evaluated at frequency ω. $\mathcal{F}^\nu$ is the Lorentz local field factor at frequency ν given by $(n_\nu^2 + 2)/3$. $\mathcal{F}^0$ is the local field factor at zero frequency, and in terms of Onsager's theory it is given by $\epsilon(n^2 + 2)/(n^2 + 2\epsilon)$. Here ϵ is the dc dielectric constant. Note that the ratio $|r_{13}/d_{13}|$ depends only negligibly on chromophore concentration, but strongly on frequencies, refractive indices at ω and 2ω, and the dc dielectric constant. The measured d_{13} and r_{13} are shown in Figure 3 as a function of DAN concentration. While both r_{13} and d_{13} depend on DAN concentration, the ratio is nearly independent of concentration as shown in Figure 3. Thus, although Onsager's theory for the local field $\mathcal{F}^0$ may not be accurate[15] the inaccuracy of $\mathcal{F}^0$ does not significantly affect the $|r_{13}/d_{13}|$ ratio, which is approximately equal to 0.46. Despite crude approximations, one notes that the calculated values agree well with the experimental ones for this model system. (See Table 1.)

B. Second-Harmonic Generation. The SHG signal (I_{SHG}) has been investigated as a function of the poling field strength for various NLO chromophore concentrations. Shown in Figure 4 is the plot of the SHG signal (for 10 wt % DNA in PMMA at 84 °C) versus E_p^2, the square of the strength of the electric field. To determine the value of E_p, we used the film thickness data, determined from the wave-guiding experiment using the Metricon, which simultaneously provides the refractive index and film thickness data. In the (0.4–1.3) × 10^6 volt/cm range, I_{SHG} appears to vary linearly with the poling field as E_p^2. Our result shows that a certain minimum poling field is needed to induce the macroscopic polarization for SHG, as indicated by the dotted extrapolated line. Similar results were found previously.[30]

To obtain the magnitude of the second-order susceptibility, we follow Jerphagnon and Kurtz[20] and obtain, for an isotropic film subject to a poling field in the direction perpendicular to the film surface, the transmitted SHG $I_{2\omega}$ excited with the incident fundamental beam at frequency ω in the p polarization as

$$I_{2\omega} = \frac{(8\pi)^3}{c} t_0^2 I_\omega^2 \chi_{\text{eff}}^{(2)}(\phi) \frac{T_{2\omega}(\phi)}{(n_\omega^2 - n_{2\omega}^2)} \sin^2\left(\frac{\pi \ell}{2\ell_c}\right) \quad (6)$$

where c is the velocity of light in vacuum and t_0 is the transmission coefficient of the second-harmonic light through the substrate. I_ω is the intensity of the fundamental beam inside the medium. $T_{2\omega}(\phi)$ is the transmission factor given by

$$T_{2\omega}(\phi) = \frac{2n_{2\omega}\cos\phi_{2\omega}'(n_\omega\cos\phi + n_0\cos\phi_\omega')(n_{2\omega}\cos\phi_\omega' + n_\omega\cos\phi_{2\omega}')}{(n_{2\omega}\cos\phi + n_0\cos\phi_{2\omega}')^2(n_{2\omega}\cos\phi + n_0\cos\phi_{2\omega}')} \quad (7)$$

where ϕ is the angle of incidence and ϕ_ν' is the refractive angle at frequency ν in the medium, and n_ω and $n_{2\omega}$ are refractive indices of the material at the fundamental and second-harmonic frequencies.

In eq 6 the effective second-order nonlinear susceptibility, $\chi_{\text{eff}}^{(2)}$ is given by

$$\chi_{\text{eff}}(2) = |\chi_{31}^{(2)}\sin\phi_\omega'\cos\phi_\omega'\cos\phi_{2\omega}' + (\chi_{33}^{(2)}\sin^2\phi_\omega' + \chi_{31}^{(2)}\cos^2\phi_\omega')\sin\phi_{2\omega}'| \quad (8)$$

By measuring the SHG intensity as a function of incident angle and fitting the result to eq 6, with the help of eqs 7 and 8 we have determined the χ_{13} and χ_{33} values for DAN in PMMA as a function of DAN concentration. The two SHG susceptibility elements $\chi_{31}^{(2)}$ and $\chi_{33}^{(2)}$ are related to the polar orientational order parameters (POP) $L_{31} = {}^1/_2 a(\langle\cos\theta_1\rangle - \langle\cos^3\theta_1\rangle)$ and $L_{33} = a\langle\cos^3\theta_1\rangle$ by[22]

$$\chi_{31}^{(2)} = \rho\beta f_{2\omega} f_\omega^2 L_{31} \quad (9a)$$

and

$$\chi_{33}^{(2)} = \rho\beta f_{2\omega} f_\omega^2 L_{33} \quad (9b)$$

Here θ_1 is the angle of the axis of the dominant β tensor

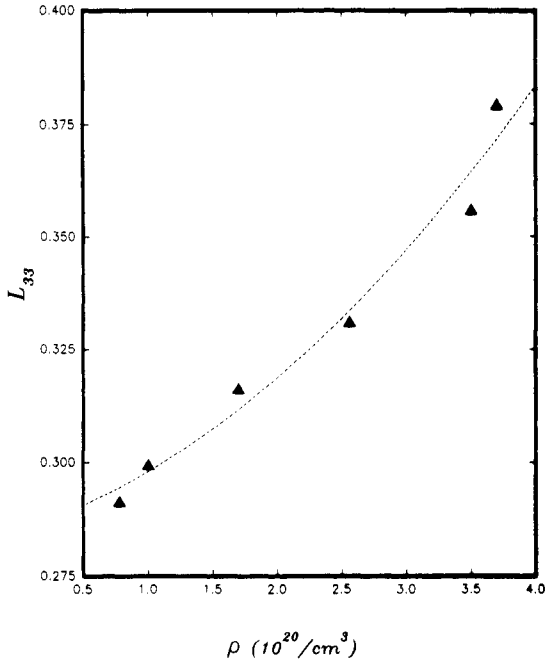

Figure 5. Polar orientational order parameter L_{33} plotted versus ρ, the number density of DAN in PMMA.

component of a representative chromophore with respect to the poling field; ρ is the number density of the (NLO) chromophores.

For a system of noninteracting NLO chromophores, the two POP's are simply given in terms of the Langevin function of order 1 and 3. In the independent dipole reorientation model, the orientation of the dipoles is completely dictated by the external field, and the polar order parameters L_{31} and L_{33} are practically independent of the concentration of the NLO chromophores, due to the fact that in this approximation the potential energy of the interaction of the NLO molecules does not play a role in affecting the values of POP.

As mentioned above, we have measured the SHG intensities versus ϕ incident angle and determined the NLO susceptibilities $\chi_{33}^{(2)}$ and $\chi_{31}^{(2)}$ by fitting to eq 7. Having obtained the values, we can calculate the POP L_{33} and L_{31}, using eqs 9a and 9b. We have found that both L_{33} and L_{31} depend on the NLO chromophore concentration. This result is similar to that previously reported found in the MNA/PMMA (MNA, 2-methyl-4-nitroaniline) system.[15] In Figure 5, we have plotted L_{33} (calculated by 9b) as a function of the DAN concentration (in number density). The β value that was needed for calculating L_{33} (cf. eq 9) was obtained from the paper by Eaton.[23] One notes that over the concentration range of 1×10^{20} to 3.7×10^{20} chromophores/cm^3, L_{33} increases from 0.28 to 0.38. The concentration dependence shows that the independent dipole orientation model described by the Langevin functions is inadequate.

As recently shown in our laboratory,[22] the concentration dependence of POP can be considered as due to the orientational pair correlation that arises from the angular dependence, or anisotropic intermolecular potential between NLO chromophores. While any type of anisotropic intermolecular potential (whether it be short- or long-range interaction) can affect the POP induced by the external electric field, due to large dipole moments of NLO chromophores the dipole–dipole interaction is believed to make the most important contribution because of its long range interaction.

In the case of the weak field poling condition, it can be shown that[22]

$$L_{33} = a(1 + \rho G_\Delta)/5 \tag{10a}$$

and

$$L_{31} = a(1 + \rho G_\Delta)/15 \tag{10b}$$

where the quantity a is equal to $\mu E_p/kT$. Here μ is the ground-state dipole moment. G_Δ is the cluster integral associated with the solution of the molecular pair correlation function. In the case of the dipole–dipole interaction, the cluster integral can be related to the Kirkwood g-factor. Since the cluster integral G_Δ also depends on ρ and is in general positive,[24] one expects L_{33} (or L_{31}) to increase with increasing the NLO chromophore density, consistent with the result of Figure 5.

C. Orientational Relaxation. Orientational pair correlation not only affects the magnitude of the NLO susceptibility, it also affects the relaxation behavior of the NLO susceptibility. The relaxation behavior is directly associated with the temporal stability of the nonlinear optical effect. We have studied this relaxation behavior. In this work the sample is first equilibrated at a chosen temperature (75 °C for that of Figure 6) and then the poling field is applied. After the SHG signal reaches a stable maximum value at a fixed poling field, the poling field is then switched off and the electrodes are shorted.

The relaxation curve shows an initial drop in intensity, followed by a gradual slower decay. The initial drop is closely related to the switching off time and is believed to be related to the decay associated with surface charge and injected space charge. The long decay portion is found sensitive to the temperature variation and also depends on the sample annealing time and the poling field strength.[30] The entire SHG signal decay cannot be fit to a single exponential. Different functional forms have been used to fit the decay shape of the guest–host[25,26] and the chromophore-functionalized NLO polymer.[27] While including the short time portion, we have fitted the SHG signal to a double Kohlraush–Williams–Watts (KWW) function[28]

$$d_{33} = {}^1/_2\chi_{33}^{(2)} = ae^{-(t/\tau_1)^{\beta_1}} + be^{-(t/\tau_2)^{\beta_2}} \tag{11}$$

We do this simply to avoid imposition of any bias imposed on the nature of the multiplicity of relaxation times for each decay mechanism. We let the computer fitting program dictate the best fit to the experimental curve. All best fits that have been obtained appear to give $\beta_1 \approx \beta_2 \approx 1$, thus indicating a biexponential decay, as shown in Figure 6.

Our results for the contact electrode poled film show that a biexponential function (i.e. setting $\beta_1 = \beta_2 = 1$ in eq 11) rather than a single KWW stretched exponential better describe the SHG decay curves. Hampsch et al.[29] who have found for the corona-poled films, the biexponential function gives a better fit. However, owing to the persistence of surface charges in the corona-poled films which tend to prolong the decay, the present results obtained by using the contact electrode-poled film with the electrodes shorted out right after turning off the poling field, is not complicated by the presence of the surface charges.[31] Actually, for the corona-poled films the result obtained in our laboratory favors the single KWW fit.[31]

While the characteristic relaxation time τ_1 is related to the decay of surface and space charges associated with the poling field, the value of τ_2 decreases rapidly as the temperature of the sample increases. Over the 55–105 °C temperature region for the 10 wt % sample, τ_2 increases

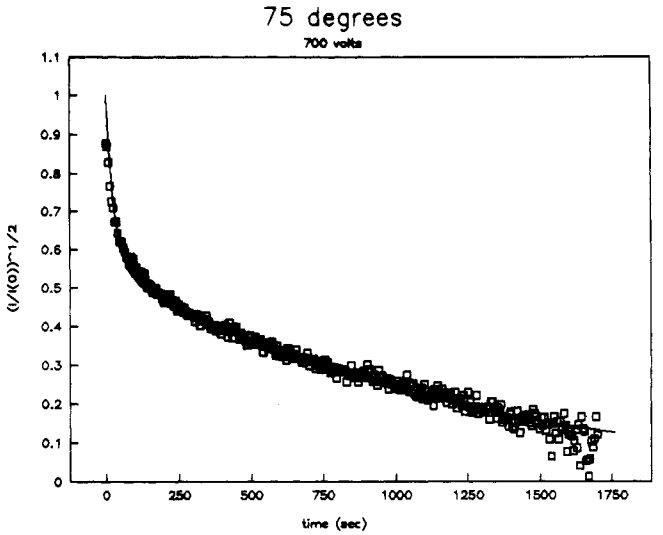

Figure 6. Relaxation of the SHG signal at 75 °C for a 5 wt % sample of DAN/PMMA, with an electric field of 0.89×10^6 V/cm. Equation 11 was used for the fit.

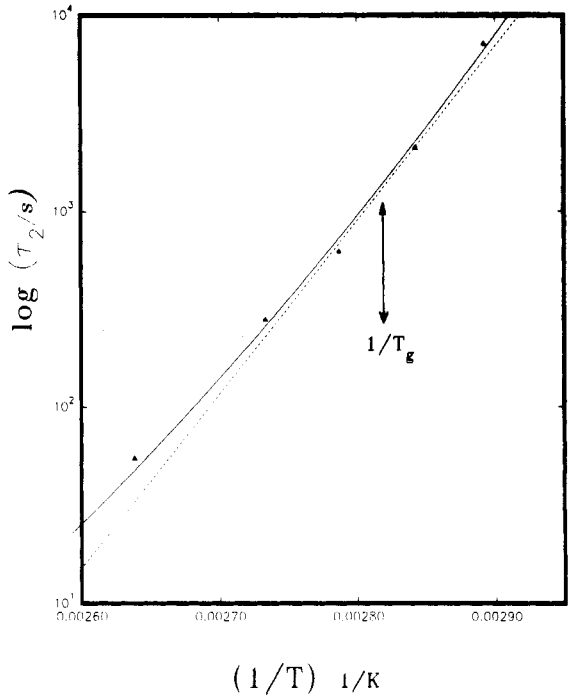

Figure 7. Plot of the slow-component relaxation time decay constants versus $1/T$. The dotted line is the Arrhenius plot, and solid line is the VFT equation fit.

from 27 s at 105 °C to 4602 s at 55 °C. For measurements below and in the vicinity of T_g (79 °C for the case of a 10 wt % DAN/PMMA sample), the relaxation time τ_2 is also affected by physical aging of the polymer.[32] The effect of physical aging on τ_2 is reported elsewhere. In Figure 7 the relaxation time τ_2 is plotted versus $1/T$ for the 10 wt % DAN in PMMA. Clearly the temperature variation of τ_2 is not Arrhenius. (The Arrhenius plot is contrasted by the dashed line.) The temperature dependence of τ_2 can be fit (shown in Figure 7) to the Vogel–Fulcher–Tammen (VFT) equation given by[33]

$$\tau_2 = \tau_\infty \exp\{B/(T - T_0)\} \qquad (12)$$

where τ_∞ is the high-temperature asymptotic relaxation time and B and T_0 are constants equal to 1405 K and 213 K, respectively.

One notes that below T_g, the α motion is in general frozen. However, because of the plasticization of the

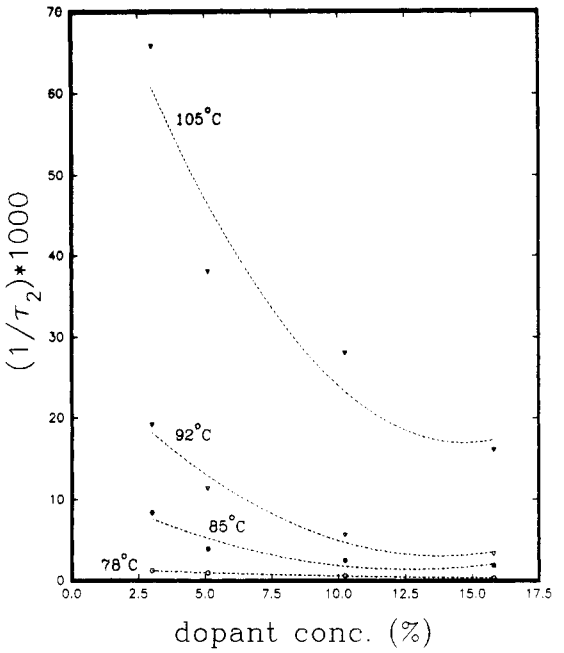

Figure 8. Concentration dependence of the slow-component relaxation times taken at various temperatures. The dotted curve is drawn to guide the eye, and each curve represents a different temperature where (▼) is 105 °C, (▽) is 92 °C, (●) is 85 °C, and (○) is 78 °C.

polymer matrix by the NLO chromophores (10 wt % in the present case), local free volume surrounding each chromophore is still sufficient to permit dipolar reorientation even at temperatures below T_g.[34] Unless considerable time is allowed to anneal the sample to uniformly distribute the chromophores, there is still room for mobility within the system. As a result, the glass transition of the amorphous guest–host system exerts little effect on τ_2; hence τ_2 undergoes a continuous change with temperature as T_g is transversed. This situation is similar to translational diffusion of photochromic dyes in the plasticized polymer matrix in the vicinity of T_g,[35,36] in which no evidence of an abrupt change in the translational diffusion coefficient is discerned as T_g is traversed, in contrast to the case of unplasticized polymer matrix.[35]

D. Concentration Dependence of Orientational Relaxation. The inverse relaxation time $(\tau_2)^{-1}$ extracted from fitting the decay of the nonlinear optical susceptibility d_{33} in accordance with eq 11 is plotted in Figure 8 as a function of NLO chromophore concentration. The data points represent values obtained for films at different concentrations and at various temperatures and poled at a field of 500 V. Interestingly, for this model system one notes that τ_2 increases with increasing NLO chromophore concentration, thereby suggesting that the increase in the loading of the NLO chromophore density slows down the SHG signal relaxation and thus enhances the stability.

In general, doping the polymer with small molecules plasticizes the polymer and lowers its glass transition temperature. For example, doping 5 wt % of DAN in amorphous PMMA depresses the T_g from 107 to 87 °C (cf. Table 1). Lowering the T_g increases the mobility of the NLO chromophore, and thus we expect τ_2 to decrease with increasing chromophore concentration. This is contrary to the result shown in Figure 8, which indicates that τ_2 steadily increases with increasing chromophore concentration. The increase of τ_2 with increasing ρ is consistent with the presence of the orientational pair correlation factor introduced above. It can be shown that τ_2 is related

to the reorientational mobility m and orientational pair correlation factor by[37]

$$\tau_2 = (1 + \rho G_\Delta)/m \quad (13)$$

where ρG_Δ represents the orientational pair correlation factor introduced previously; the mobility m is related to the dynamic orientational pair correlation factor and the reorientational relaxation time of an uncorrelated NLO chromophore. If the mobility is not strongly affected by the chromophore concentration, one will expect τ_2 to increase with the chromophore concentration. This situation is quite similar to light scattering in which the reciprocal of the line width of the depolarized Rayleigh spectrum of a system of optically anisotropic molecules is proportional to the orientational relaxation time τ_R,[38] where the orientational relaxation time τ_R is affected by both the static and dynamic orientational pair correlation in a manner similar to that described by eq 13. However, in the present situation, we are concerned with the orientational relaxation associated with the polar order L_{33}, rather than the quadrupolar order involved in light scattering.

IV. Conclusions

In conclusion, both the linear electrooptic Pockels effect and second-harmonic generation have been used to study the polar orientational order of a model guest–host polymeric system. We have found both the Pockels coefficient r_{13} and second-harmonic coefficient d_{13} show a nonlinear relationship with respect to the concentration of DAN in PMMA. A relation based on a two level has been used to convert linear electrooptic coefficients to the second-order nonlinear susceptibilities. Despite the crude approximation introduced in the model the calculated values have been found to yield good agreement with measured ones. The orientational order parameter has been obtained from the $\chi^{(2)}$ measurements for six different NLO concentrations and has been found to increase with increasing chromophore concentration. The temperature dependence of the decay has been found to follow the VFT equation. The concentration dependence on the orientational decay is attributed to orientational pair correlation associated with intermolecular interactions.

Acknowledgment. We thank the Office of Naval Research for providing financial support for this work. T.G. acknowledges the Harris Foundation for a fellowship. We also thank Mr. H. W. Guan for providing technical assistance.

References and Notes

(1) Stahelin, M.; Walsh, C. A.; Burland, D. M.; Miller, R. D.; Twieg, R. J.; Volksen, W. *J. Appl. Phys.* **1993**, *73* (12), 8471.
(2) Lytel, R.; Lipscomb, G. *Mater. Res. Soc. Symp. Proc.* **1992**, *247*, 17.
(3) Eich, M.; Sen, A.; Hesser, H.; Bjorklund, G. C.; Swalen, J. D.; Twieg, R. J.; Yoon, D. Y. *J. Appl. Phys.* **1989**, *66*, 2559.
(4) Eich, M.; Bjorklund, G. C.; Yoon, D. Y. *Polym. Adv. Technol.* **1990**, *1*, 189.
(5) Ye, C.; Minami, N.; Marks, T. J.; Yand, J.; Wong, G. K. *Macromolecules* **1988**, *21*, 2899.
(6) Chen, M.; Yu, L.; Dalton, L.; Shi, Y.; Steier, W. *Macromolecules* **1991**, *24*, 5421.
(7) Mandal, B.; Chen, Y.; Lee, J.; Kumar, J.; Tripathy, S. *Appl. Phys. Lett.* **1991**, *58*, 2459.
(8) Wu, J.; Valley, J.; Ermer, S.; Binkley, E.; Kenney, J.; Lytel, R. *Appl. Phys. Lett.* **1991**, *59*, 2213.
(9) Stahelin, M.; Burland, D. M.; Ebert, M.; Miller, R. D.; Smith, B. A.; Twieg, R. J.; Volksen, W.; Walsh, C. A. *Appl. Phys. Lett.* **1992**, *61*, 1626.
(10) Valley, J.; Wu, J.; Ermer, S.; Stiller, M.; Binkley, E.; Kenney, J.; Lipscomb, G.; Lytel, R. *Appl. Phys. Lett.* **1992**, *60*, 160.
(11) Zyss, J.; Chemla, D. S.; Nicoud, J. F. *J. Chem. Phys.* **1981**, *74*, 4800.
(12) Wang, C. H.; Guan, H. W.; Zhang, J. F. *Proc. SPIE* **1991**, *1559*, 39.
(13) Kunz, K. S. *Am. J. Phys.* **1977**, *45*, 267.
(14) Hirschmann, H.; Meier, W.; Finkelmann, H. *Proc. SPIE* **1991**, *1559*, 27.
(15) Guan, H. W.; Wang, C. H. *J. Chem. Phys.* **1993**, *98*, 3463.
(16) Meier, W.; Finkelmann, H. *Makromol. Chem. Rapid Commun.* **1990**, *11*, 599.
(17) Forsbergh, P. W. *Handbuch der Physik*; Springer Verlag: Berlin, 1956; p 289.
(18) Oudar, J. L.; Chemla, D. S.; Batifol, E. *J. Chem. Phys.* **1977**, *67*, 1626.
(19) Oudar, J. L. *J. Chem. Phys.* **1977**, *67*, 446.
(20) Jerphagnon, J.; Kurtz, S. K. *J. Appl. Phys.* **1970**, *41*, 1667.
(21) LeGrange, J. D.; Kuzyk, M. G.; Singer, K. D. *Mol. Cryst. Liq. Cryst.* **1987**, *1606*, 567.
(22) Wang, C. H. *J. Chem. Phys.* **1993**, *98*, 3457.
(23) Eaton, D. F. Nonlinear Optical Materials, The Great and Near Great, beta value is 36 esu × 10^{30}. E.I. du Pont de Nemours and Company, research report.
(24) Hansen, J. P.; McDonald, I. R. *Theory of Simple Liquids*, 2nd ed.; Academic Press: San Diego, CA, 1986.
(25) Goodson, T., III; Wang, C. H. *Macromolecules* **1993**, *26*, 1837.
(26) Knabke, G.; Franke, H. *Appl. Phys. Lett.* **1991**, *58*, 678–680.
(27) Stahelin, M.; Walsh, C. A.; Burland, D. M.; Miller, R. D.; Twieg, R. J.; Volksen, V. *J. Appl. Phys.* **1993**, *73*, 8471.
(28) Williams, G. *Adv. Polym. Sci.* **1979**, *33*, 461.
(29) Hampsch, H. L.; Yang, J.; Wong, G. K.; Torkelson, J. M. *Macromolecules* **1988**, *21*, 526.
(30) Guan, H. W.; Wang, C. H.; Gu, S. H. *J. Chem. Phys.*, in press.
(31) Wang, C. H.; Gu, S. H.; Guan, H. W. *J. Chem. Phys.* **1993**, *99*, 5597.
(32) Struvik, C. E. Physical Aging in Amorphous Polymers and Other Materials; Elsevier: Amsterdam, 1978.
(33) Ferry, J. *Viscoelastic Properties of Polymers*; Wiley: New York, 1961; p 201.
(34) Fujita, H. *Polymer Solutions*; Elsevier: Oxford, 1990; p 235.
(35) Wang, C. H.; Xia, J. L.; Yu, L. *Macromolecules* **1991**, *24*, 3638.
(36) Zhang, X. Q.; Wang, C. H. *J. Polym. Sci., Polym. Phys. Ed.* **1994**, *32*, 569.
(37) Wang, C. H. To be submitted for publication.
(38) Berne, B.; Pecora, R. *Dynamic Light Scattering*; Wiley: New York, 1976.